Distributed Adaptive Prescribed Performance Control for Interconnected Euler-Lagrange Systems under Input Constraints

Tian Tao[1], Charalampos P. Bechlioulis[2], Dimos V. Dimarogonas[1]

***Abstract*—This paper proposes a novel distributed adaptive Prescribed Performance Control (PPC) scheme with low complexity for interconnected multi-input multi-output (MIMO) Euler-Lagrange systems subject to structural uncertainty in dynamics, input saturation, and external disturbances without employing any approximation structures. In addition to the coupling caused by the control protocol, uncertain nonlinear interconnection terms intrinsically existing in the dynamics are also considered. The control scheme is implemented in a distributed manner among multiple agents, utilizing only local information. Adaptive control tools are employed to introduce flexible prescribed performance functions, which serve as a trade-off between input and output constraints, effectively dampening the input saturation and eliminating the need for an auxiliary system. The proposed approach is analyzed using Lyapunov techniques, and is validated by simulation results on a leader-follower multi-agent trajectory tracking control problem.**

I. Introduction

Prescribed Performance Control (PPC) is a method that deals with user-defined attributes of transient and steady-state performance. It was first proposed in [1] and has been widely used in various applications such as water tanks [2], robot manipulators [3], and UAV formation control [4]. The uncertainties that arise in PPC can be classified into two types: *parametric uncertainty* [5] and *structural uncertainty* [6]–[8], originating from unmodelled dynamics or unknown system nonlinearities. To address the latter type of uncertainty, approximation-based approaches are utilized in [1], increasing the complexity of the controller design. In [9] the PPC of uncertain Euler-Lagrange systems with input saturation is tackled via neural network approximation, but the accuracy of this approach is sensitive to the initial randomization of the weight matrices.

On the one hand, the majority of the existing literature on PPC implements the controller in a centralized manner in a single-agent system with no uncertainty [10], parametric uncertainty [5], or structural uncertainty [6]–[8], [11]. The interaction among multiple agents is caused not only by sensing or communication but also by physical interconnections. However, there is not much research on multi-agent PPC [12], which accounts for the connection among multiple agents due to control protocols through sensing or communication [13]–[16]. Internal connections that intrinsically exist in the dynamics through physical interconnection before the control protocol is applied are often neglected in multi-agent work. A typical example of such intrinsic interaction is power flow due to phase difference through tie-lies that physically connect multiple areas in smart grids [17]. Only a few studies consider the intrinsic interconnections in multi-agent PPC subject to structural uncertainty and external disturbance. One exception is [18], which accounts for physical interaction and parametric uncertainties without external disturbances. Therefore, there is still a need to address the challenge of dealing with intrinsic interconnections in multi-agent PPC research under structural uncertainties and external disturbances.

On the other hand, input saturation of the actuator can limit the control effort that can be exerted on the system, which may cause the aforementioned literature to fail [13]–[16]. A linear multi-input multi-output (MIMO) system [19], a nonlinear single-input single-output (SISO) system [20]–[24], and a nonlinear MIMO system [25] with input saturation are studied by PPC controllers in a centralized manner within a single-agent framework. In order to strike a balance between input and output constraints, a modified performance function (MPF) is first proposed via an auxiliary system in [26], leading however to a high-complexity control design [20]–[22], [27]. Accurate full knowledge of the dynamics is required for many input-constrained PPC papers, which is further improved by considering uncertainty in the dynamics for first-order input-constrained PPC system in [28], for high-order ones in [29], [30]. An uncertain Euler-Lagrange system subject to input saturation under adaptive sliding mode control is studied in [31] without considering prescribed performance. The uncertainties in input-constrained PPC are solved via neural network approximation within a single-agent framework in [9], via fuzzy system approximation within a single-agent framework in [20]–[22] and within a multi-agent framework for stochastic system in [32]. All of this input-constrained PPC work is implemented in a centralized way (except [32]), requiring global information without considering intrinsic interconnections.

In conclusion, input-constrained distributed PPC in the presence of structural uncertainty, intrinsic interconnection, and external disturbance still lacks adequate study. The main challenge we address is that existing PPC is typically designed either for a single agent often in a SISO configuration, or without considering input constraints, or utilizing auxiliary system to compensate the input saturation, or requesting exact knowledge of the dynamics, or utilizing approximation-based control in the presence of uncertainty. The combination of all these issues we deal with has not been addressed in existing PPC work due to several technical difficulties: 1) Input saturation must be compensated for, often necessitating

This work was supported by the KAW (Knut & Alice Wallenberg (KAW) foundation and the Swedish Research Council (VR). The work of C.P.B. was supported by the Hellenic Foundation for Research and Innovation (H.F.R.I.) under the second call for research projects to support postdoctoral researchers (HFRI-PD19-370).

Tian Tao and D. V. Dimarogonas are with the Division of Decision and Control Systems, KTH Royal Institute of Technology, Stockholm, Sweden (tiantao@kth.se,dimos@kth.se).

C. P. Bechlioulis is with the Department of Electrical and Computer Engineering, University of Patras, Greece (chmpechl@upatras.gr).

the use of auxiliary systems in many input-constrained PPC, leading to a more complex control design; 2) The presence of uncertainty in dynamics complicates control design, often resulting in the need for approximation-based control methods; 3) A multi-agent system in MIMO configuration is more complex compared to single-agent system in SISO configuration, and distributed control can only utilize local information. When integrating all of these elements into a single controller, a complex control design may be necessary, as it requires the auxiliary system and approximation approach along with global information. Motivated by this challenge, this paper aims to propose an adaptive distributed control scheme that synchronizes unknown interconnected Euler-Lagrange systems while meeting prescribed transient and steady-state performance. The main contributions are given as follows: 1) the low-complexity controller operates in a distributed manner only requiring local information in the multi-agent MIMO system; 2) the intrinsic coupling terms in dynamics are taken into account before the control protocol is applied; 3) an adaptive prescribed performance function is introduced, which relaxes when the inputs saturation occurs and recovers when the input saturation vanishes, without the need for an auxiliary system; 4) neither an upper bound on the structural uncertainty nor an approximation is required in the presence of structural uncertainty in the dynamics.

The rest of the paper is organized as follows: Section II describes the uncertain dynamics and formulates the problem; Section III presents the distributed control design with adaptive PPC; Section IV includes Lyapunov stability analysis, and Section V provides a simulation study, followed by concluding remarks in Section VI.

We adopt a standard notation, with $\mathbb{R}^+$ for the set of positive real numbers, $\mathbb{R}^n$ for the n-dimensional vector, $\otimes$ for the Kronecker product, I_N for the identity matrix of dimension N, $\underline{1}_N$ for the N-dimensional vector of ones, $\underline{0}_N$ for the N-dimensional vector of zeros, $\underline{\sigma}(\cdot)$ and $\overline{\sigma}(\cdot)$ for the minimum and maximum singular value of a matrix, and $\|\cdot\|$ for the Euclidean norm.

II. Problem Formulation

A. System Description

Consider a group of agents with a leader and N followers. The dynamic model for each follower is described by an Euler-Lagrange system with n inputs and n outputs:

$$\begin{aligned} &M^i(q^i)\ddot{q}^i + C^i(q^i,\dot{q}^i)\dot{q}^i + G^i(q^i) \\ &+ H^i(q^i,q^j,\dot{q}^i,\dot{q}^j) + F^i(\dot{q}^i) + d^i(t) = \tau^i \end{aligned} \tag{1}$$

where $q^i = [q^i_1,\ldots,q^i_n]^T \in \mathbb{R}^n, \dot{q}^i = [\dot{q}^i_1,\ldots,\dot{q}^i_n]^T \in \mathbb{R}^n$, and $\ddot{q}^i = [\ddot{q}^i_1,\ldots,\ddot{q}^i_n]^T \in \mathbb{R}^n$ are the generalized coordinates and their derivatives, and $\tau^i \in \mathbb{R}^n$ are the control inputs for $i = 1,\ldots,N$. The system dynamics (1) comprises the mass/inertia matrix $M^i(q^i) : \mathbb{R}^n \to \mathbb{R}^{n\times n}$, the centripetal term $C^i(q^i,\dot{q}^i) : \mathbb{R}^{n\times n} \to \mathbb{R}^{n\times n}$, the gravity term $G^i(q^i) : \mathbb{R}^n \to \mathbb{R}^n$, and , the friction term $F^i(\dot{q}^i) : \mathbb{R}^{n\times n} \to \mathbb{R}^n$. In addition, $H^i(q^i,q^j,\dot{q}^i,\dot{q}^j) : \mathbb{R}^n \times \mathbb{R}^n \times \mathbb{R}^n \times \mathbb{R}^n \to \mathbb{R}^n$ are the coupling terms between agent i and other agents $j \in \{1,\ldots,N\}$ caused by intrinsic physical interconnections that exist in dynamics before the control protocol is applied. In addition, $d^i(t) \in \mathbb{R}^n$ denote unknown but bounded and piecewise continuous external disturbances, i.e. $\|d^i(t)\| \leq \bar{d}^i, \forall t$ with unknown bounds $\bar{d}^i$. In the dynamics, $M^i(q^i), C^i(q^i,\dot{q}^i), G^i(q^i), F^i(\dot{q}^i), H^i(q^i,q^j,\dot{q}^i,\dot{q}^j)$ are the structural uncertainties. The difference between structural and parametric uncertainties is whether the mathematical structure is known. For example, the elements of the system matrices $M^i(q^i)$ are unknown. And $\tau_i = [\tau^i_1,\ldots,\tau^i_n]^T \in \mathbb{R}^n$ are the generalized control inputs subject to input saturation as follows:

$$\tau^i_k = \mathrm{sat}(u^i_k) = \begin{cases} u^i_k, |u^i_k| < \bar{u}^i_k, \\ \bar{u}^i_k \,\mathrm{sgn}(u^i_k), |u^i_k| \geq \bar{u}^i_k. \end{cases} \tag{2}$$

where the symbol $\mathrm{sgn}(\cdot)$ denotes the sign function and $\bar{u}^i_k > 0$ represents the maximum input level for the kth dimension of the ith agent for $k = 1,\ldots,n$, and $i = 1,\ldots,N$. Such input constraints restrict the actuator's control over the system.

The communication between the group of N followers can be modeled by a directed graph $\mathcal{G} = (\mathcal{V},\mathcal{E})$, where the set of vertices $\mathcal{V} = \{v_1,...,v_N\}$ denotes the followers and the set of communication edges $\mathcal{E} \subseteq \mathcal{V} \times \mathcal{V}$ represents the path of information exchange between two distinct vertices. The adjacency matrix $A = [a_{ij}] \in \mathbb{R}^{N\times N}$ associated with $\mathcal{G}$ attains $a_{ij} = 1$ if agent i has access to the state-information of agent j (i.e. $(v_j,v_i) \in \mathcal{E}$), otherwise $a_{ij} = 0$ (i.e., $(v_j,v_i) \notin \mathcal{E}$). The Laplacian matrix $\mathcal{L} = [l_{ij}] \in \mathbb{R}^{N\times N}$ associated with $\mathcal{G}$ is defined as $l_{ii} = \sum_{j=1,j\neq i}^N a_{ij}$ and $l_{ij} = -a_{ij},\ i \neq j$. It is known that $\mathcal{L}\underline{1}_N = \underline{0}_N$ [33]. The access of the follower nodes to the leader is represented by a diagonal matrix $B = \mathrm{diag}([b_1,b_2,...,b_n]) \in \mathbb{R}^{N\times N}$ where $b^i = 1$ means that the ith follower node v_i can obtain state-information from the leader node v_0; otherwise $b^i = 0, i \in \{1,2,...,N\}$. The augmented communication graph is defined as $\bar{\mathcal{G}} = (\bar{\mathcal{V}},\bar{\mathcal{E}})$, where $\bar{\mathcal{V}} = \{v_0,v_1,...,v_N\}$ and $\bar{\mathcal{E}} = \mathcal{E} \cup \{(v_i,v_0) : b_i = 1\} \subseteq \bar{\mathcal{V}} \times \bar{\mathcal{V}}$.

Lemma 1. *[34] The Kronecker product $\otimes$ has the following properties: For matrices A, B, C, and D of appropriate dimensions, (1) $A \otimes C + B \otimes C = (A + B) \otimes C$; (2) $(A \otimes B)(C \otimes D) = (AC) \otimes (BD)$.*

Given the state of the leader $q^0 = [q^0_1,\ldots,q^0_n] \in \mathbb{R}^n$ that generate a reference trajectory with unknown dynamics, define $\delta = (q - \underline{q}^0) \in \mathbb{R}^{nN}$ as the global synchronization error concerning the leader with $q = [q^1,\ldots,q^N]^T \in \mathbb{R}^{nN},\ \underline{q}^0 = \underline{1}_N \otimes q^0 \in \mathbb{R}^{nN}$.

Problem Formulation. *Consider uncertain interconnected Euler-Lagrange systems* (1) *subject to input saturation* (2)*, structural uncertainty, intrinsic couplings, and external disturbances. Design distributed controllers $u^i_k(t)$, in the sense that only local information (the state-information of agent i and its communication neighboring agents) can be used for $k = 1,\ldots,n$ and $i = 1,\ldots,N$, such that all the follower agents track the leader's trajectory, i.e., the global synchronization error δ evolves within a predefined and arbitrarily small boundary around the origin.*

To address the synchronization problem for multi-agent systems (MAS), the following assumption is a standard condition in directed graphs [14].

Assumption 1. *The augmented communication graph $\bar{\mathcal{G}}$ contains a spanning tree with the root being the leader node.*

Assumption 1 ensures that a directed path from the leader to any follower node exists. Similar to the definition of the communication graph $\mathcal{G}$ among N followers, we also provide the definition of the intrinsic interconnection graph among N followers, denoted as $\mathcal{G}' = (\mathcal{V}', \mathcal{E}')$. The set of vertices $\mathcal{V}' = \{v_1, ..., v_N\}$ denotes the followers, and the set of connection edges $\mathcal{E}' \subseteq \mathcal{V}' \times \mathcal{V}'$ represents the path of physical interconnection between two distinct vertices. The neighboring agents of agent i with respect to *communication topology* $\mathcal{G}$ and *physical interconnection topology* $\mathcal{G}'$ are denoted by sets $\mathcal{N}_i = \{1, \dots, N\}$ and $\mathcal{N}_i' = \{1, \dots, N\}$, respectively. Notably, Assumption 1 involves only the communication topology $\mathcal{G}$, not the physical topology $\mathcal{G}'$ as shown in Fig. 1.

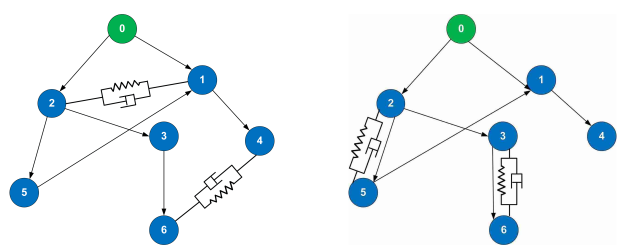

(a) Interconnection 1 (b) Interconnection 2

Figure 1: Topology of networks (the solid line represents the edges of communication topology, and the spring-damper represents the edges of physical topology).

Assumption 2. *$H^i(q^i, q^j, \dot{q}^i, \dot{q}^j)$ are locally Lipschitz functions, satisfying $||H^i(q^i, q^j, \dot{q}^i, \dot{q}^j)|| \leq \bar{h}_0||q^i|| + \bar{h}_0'||q^j|| + \sum_{j\in\mathcal{N}_i'}\left(\bar{h}_j||\dot{q}^i|| + \bar{h}_j'||\dot{q}^j||\right)$ with unknown constants $\bar{h}_0, \bar{h}_0', \bar{h}_j, \bar{h}_j' \in \mathbb{R}^+, j \in \mathcal{N}_i'$.*

Assumption 3. *As common in EL literature [35], the desired trajectory q^0 is an unknown continuously differentiable and bounded function of time with bounded but unknown first derivative $\dot{q}^0$ and second derivative $\ddot{q}^0$.*

Let us now define the tracking error $e^i(t) = [e_1^i, \dots, e_n^i]^T \in \mathbb{R}^n$ and its derivative $\dot{e}^i = [\dot{e}_1^i, \dots, \dot{e}_n^i]^T \in \mathbb{R}^n$ for $i = 1, \dots, N$ and $k = 1, \dots, n$ as follows:

$$e_k^i = \sum_{j\in\mathcal{N}_i} a_{ij}(q_k^i - q_k^j) + b^i(q_k^i - q_k^0) \tag{3a}$$

$$\dot{e}_k^i = \sum_{j\in\mathcal{N}_i} a_{ij}(\dot{q}_k^i - \dot{q}_k^j) + b^i(\dot{q}_k^i - \dot{q}_k^0) \tag{3b}$$

where $q_k^0,\ \dot{q}_k^0 \in \mathbb{R}$ represent the kth state variable of the leader and its derivative, $k = 1, \dots, n$. The leader's state q^0, and its derivative $\dot{q}^0$ are bounded and measurable for feedback for those agents i for which $b_i = 1$.

Let us define $e = [e^1, \dots, e^N]^T \in \mathbb{R}^{nN}$, $q = [q^1, \dots, q^N]^T \in \mathbb{R}^{nN}$. Then from (3a) we have

$$e = \big((\mathcal{L} + B) \otimes I_n\big)(q - \underline{q}^0) = \big((\mathcal{L} + B) \otimes I_n\big)\delta \tag{4}$$

The detailed derivation from (3b) to (4) is provided in Appendix. Note that δ cannot be used for control design as it contains global information, i.e. the leader's state information, which is not available to all followers. Due to Assumption 1, the following lemma is known from the literature:

Lemma 2. *[14] The local and global synchronization errors are related by*

$$\|\delta\| \leq \frac{\|e\|}{\underline{\sigma}(\mathcal{L} + B)} \tag{5}$$

with $\underline{\sigma}(\mathcal{L} + B)$ being the minimum singular value of $(\mathcal{L} + B)$, which is positive for any augmented graph that satisfies Assumption 1.

The following properties for the dynamic terms in (1) are taken or further extended from the literature [36]:

Property 1. *There exist $\bar{c}^i$, $\bar{g}^i$, $\bar{f}^i \in \mathbb{R}^+$ such that $\|C^i(q^i, \dot{q}^i)\| \leq \bar{c}^i\|\dot{q}^i\|$, $\|F^i(\dot{q}^i)\| \leq \bar{f}^i\|\dot{q}^i\|$, $\|G^i(q^i)\| \leq \bar{g}^i$, i=1,…,N.*

Property 2. *The matrix $M^i(q^i)$ is symmetric and uniformly positive-definite in q^i. There exist positive constants $\underline{m}$ and $\overline{m}$ such that $0 \leq \underline{m}I_n \leq M^i(q^i) \leq \overline{m}I_n, i = 1, \dots, N$.*

All the constants in Assumption 2 and Properties 1, 2 are assumed unknown for the control design.

B. Prescribed Performance Control

The Prescribed Performance Control (PPC) technique ensures that an error remains within a predefined bound [1], described by performance functions $\rho_k^i(t)$, which are continuously differentiable and obey $\rho_k^i(0) \geq \rho_k^i(\infty) > 0$. Given initial condition $\rho_k^i(0)$, the constant $\rho_k^i(\infty) = \lim_{t\to\infty} \rho_k^i(t) > 0$ is the maximum allowable size of the error at the steady state. In our case, let us define a combined error vector $s(\tilde{e}) = [s^1, \dots, s^N]^T$, where $s^i(\tilde{e}^i) = [s_1^i, \dots, s_n^i]^T$ with $\rho_k^i(0) > |s_k^i(\tilde{e}_k^i(0))|$ are calculated by $e^i(t)$ and $\dot{e}^i(t)$ as

$$s_k^i(\tilde{e}_k^i) = \dot{e}_k^i + \alpha e_k^i \tag{6}$$

The prescribed performance bounds are given by

$$-\rho_k^i(t) {\leq} s_k^i {\leq} \rho_k^i(t) \tag{7}$$

where $\tilde{e} = [\tilde{e}^1, \dots, \tilde{e}^N]^T, \tilde{e}^i = [\tilde{e}_1^i, \dots, \tilde{e}_n^i]^T$ with $\tilde{e}_k^i = [e_k^i, \dot{e}_k^i]^T$ for $k = 0, \dots, n$, $i = 1, \dots, N$, and α is a user-defined positive constant.

Proposition 1. *[37, pp. 277] The synchronization problem is equivalent to driving the combined error $\tilde{e}(t)$ on the invariant boundary layer $S := \{\tilde{e}(t) \in \mathbb{R}^{2nN} : ||s(\tilde{e})|| \leq \bar{s}\}$ with $\bar{s}$ denoting a positive constant. If $s(\tilde{e}(0)) \in S$ then all $\tilde{e}_k^i(t), i = 1, ..., N$ and $k = 1, \dots, n$ $\forall t > 0$ are bounded with respect to compact sets whose size is determined by $\bar{s}$.*

According to Proposition 1, the bounds on scalar $s_k^i(\tilde{e}_k^i)$ in (6) can be directly translated into bounds on the vectors

$\tilde{e}^i_k$, which constitute the local position tracking errors e^i_k and local velocity tracking errors $\dot{e}^i_k$ for $k = 1, \ldots, n$ and $i = 1, \ldots, N$. Consequently, the global synchronization error δ can be bounded by the local position error e via (5). Hence, $s(\tilde{e})$ represents a valid performance metric of the synchronization control problem.

III. Adaptive PPC with input constraints

Let us define the normalized errors concerning the performance functions

$$\xi^i_{sk} = \frac{s^i_k}{\rho^i_k}. \tag{8}$$

Next, define the error transformation functions $\varepsilon^i_k(\xi^i_{sk}) = \frac{1}{2}\ln\left(\frac{1+\xi^i_{sk}}{1-\xi^i_{sk}}\right)$ where $\varepsilon^i_k : [-1, 1] \to \mathbb{R}, \forall t \in [0, T_{\max})$, as well as their derivatives $r^i_k = \frac{1}{(1-\xi^i_{sk})(1+\xi^i_{sk})}$ for $i = 1, \ldots, N$ and $k = 1, \ldots, n$. Accordingly, the distributed controllers are designed as

$$u^i_k = -\beta^i_k \varepsilon^i_k \frac{r^i_k}{\rho^i_k} \tag{9}$$

where β^i_k are the user-defined positive constants for $k = 1, \ldots, n$ and $i = 1, \ldots, N$.

Remark 1. *In traditional low-complexity PPC, a simple controller $u = -\beta\varepsilon$ is used for a single-agent SISO system in [29] and a single-agent MIMO system in [38]. In comparison to traditional low-complexity PPC, our approach includes an additional term, $\frac{r^i_k}{\rho^i_k}$, in the controller as indicated in* (9)*. The reason is explained in the following analysis:*

In traditional low-complexity PPC, a simple controller $u = -\beta\varepsilon$ in a single-agent SISO system in [29] leads to a negative term $-\varepsilon\rho^{-1}r\gamma\beta\varepsilon$ where $\varepsilon, \rho^{-1}, r, \gamma, \beta$ are scalars in the respective Lyapunov analysis. When calculating the Lyapunov function derivative $\dot{V}$, one can bound it from above by the absolute values of scalars ε, resulting in $\dot{V} \leq \frac{\varepsilon}{(1-\xi^2)\rho}(D - \gamma k\varepsilon) \leq \frac{1}{(1-\xi^2)\rho}(\bar{Z}|\varepsilon| - \gamma k|\varepsilon|^2)$. Consequently, it can be concluded that $\dot{V} < 0$ when $|\varepsilon| > \frac{\bar{Z}}{\gamma k}$.

In our work, we consider a multi-agent MIMO system, leading to a negative term $-\varepsilon^T\rho^{-1}r\gamma\beta\varepsilon$ where ρ, r, γ, β are now matrices and ε is a vector in the respective Lyapunov analysis. When calculating the Lyapunov function derivative $\dot{V}$, to apply the Rayleigh-Ritz theorem, we need to construct a quadratic form. By introducing $\frac{r^i_k}{\rho^i_k}$ into the simple controller $u^i_k = -\beta^i_k\varepsilon^i_k$ and combing it with the diagonality of matrices $\rho^{-1}, r, \gamma, \beta$, the first term of the Lyapunov function derivative $\dot{V}$ in (24) *is $-\varepsilon^T\rho^{-1}r\gamma\beta r\rho^{-1}\varepsilon = -(r\rho^{-1}\varepsilon)^T\gamma\beta(r\rho^{-1}\varepsilon) \leq -\frac{1}{2}\underline{\sigma}(\gamma\beta)\underline{\sigma}^2(\rho^{-1})\|\varepsilon\|^2 - \frac{1}{2}\underline{\sigma}(\gamma\beta)\|\varepsilon^T\rho^{-1}r\|^2$.*

The conventional fixed prescribed performance function is usually a priori defined as [38]

$$\rho^i_k(t) = (\rho^i_k(0) - \rho^i_k(\infty))\exp^{-\lambda^i_k t} + \rho^i_k(\infty), t > 0 \tag{10}$$

with $\lambda^i_k > 0$. These functions are designed to decrease exponentially at the rate λ^i_k for $i = 1, N,\ k = 1, \ldots, n$. The goal is to ensure that the combined errors s^i_k remain within a specific boundary. However, it is possible for the combined errors $s^i_k(\tilde{e}^i_k)$ to exceed this boundary due to input saturation (as described in (2)). To address this issue, the performance functions $\rho^i_k(t)$ are designed to adapt dynamically based on the activation of the input saturation as follows:

$$\dot{\rho}^i_k = -\lambda^i_k(\rho^i_k - \rho^i_k(\infty)) + \gamma^i_k \frac{\text{sat}\,(u^i_k) - u^i_k}{\xi^i_{sk}} \tag{11}$$

where γ^i_k are the user-defined positive constants for $k = 1, \ldots, n$ and $i = 1, \ldots, N$. The second term in (11) is always non-negative $\forall\xi^i_{sk} \in [-1, 1]$. Let's consider three scenarios:

a) When the combined errors s^i_k approach the upper boundary of the corresponding envelopes, we have $s^i_k > 0$. Then $\xi^i_{sk} = \frac{s^i_k}{\rho^i_k} \to 1$, $\varepsilon^i_k = \frac{1}{2}\ln\left(\frac{1+\xi^i_{sk}}{1-\xi^i_{sk}}\right) \to +\infty$, and $r^i_k = \frac{1}{(1-\xi^i_{sk})(1+\xi^i_{sk})} \to +\infty$, resulting in a negative control signal $u^i_k = -\beta^i_k\varepsilon^i_k\frac{r^i_k}{\rho^i_k} \to -\infty$ according to (9). Then the input difference $\Delta u^i_k = \text{sat}(u^i_k) - u^i_k \to +\infty$ according to (2). Consequently, the second term $\gamma^i_k\frac{\Delta u^i_k}{\xi^i_{sk}} \to +\infty$ in (11) provides a significant large relaxation of the envelope boundary by increasing ρ^i_k.

b) When the combined errors s^i_k approach the lower boundary of the corresponding envelopes, we have $s^i_k < 0$. Then $\xi^i_{sk} = \frac{s^i_k}{\rho^i_k} \to -1$, $\varepsilon^i_k = \frac{1}{2}\ln\left(\frac{1+\xi^i_{sk}}{1-\xi^i_{sk}}\right) \to -\infty$, and $r^i_k = \frac{1}{(1-\xi^i_{sk})(1+\xi^i_{sk})} \to +\infty$, leading to a negative control signal $u^i_k = -\beta^i_k\ln(\frac{1+\xi^i_{sk}}{1-\xi^i_{sk}})\frac{\varepsilon^i_k}{\rho^i_k} \to +\infty$ according to (9). Then the input difference $\Delta u^i_k = \text{sat}(u^i_k) - u^i_k \to -\infty$ according to (2). Therefore, the second term $\gamma^i_k\frac{\Delta u^i_k}{\xi^i_{sk}} \to +\infty$ in (11) provides a significant large relaxation of the envelope boundary by increasing ρ^i_k.

c) In addition to the extreme scenarios where $\xi^i_{sk} = \pm 1$ in scenarios a) and b), we can also consider the less extreme scenario where $\xi^i_{sk} \in (-1, 1)$. In this case, it is not difficult to find that the sign of $\Delta u^i_k = \text{sat}(u^i_k) - u^i_k$ and ξ^i_{sk} are always the same. Therefore, it is straightforward to conclude that $\gamma^i_k\frac{\Delta u^i_k}{\xi^i_{sk}} \geq 0,\ \forall\xi^i_{sk} \in (-1, 1)$.

Hence, the second term $\gamma^i_k\frac{\Delta u^i_k}{\xi^i_{sk}} \geq 0$ in (11) always holds $\forall\xi^i_{sk} \in [-1, 1]$, regardless of the sign of normalized error ξ^i_{sk} or Δu^i_k separately.

Some input-constrained PPC papers require the introduction of an auxiliary system to compensate for the input saturation, leading to a more complex control design [20]–[22], [26], [27]. In contrast, our paper successfully addresses input saturation using a low-complexity controller without the need for an auxiliary system. Our approach takes advantage of the adaptive performance functions in (11), which possess the following properties:

- Saturated inputs case: when the combined errors s^i_k are large enough to approach the boundary of the envelope, normalized errors $\xi^i_{sk} = \frac{s^i_k}{\rho^i_k}$ become significantly large. This leads to an increase in the transformed errors ε^i_k and r^i_k. Consequently, the input signals $u^i_k = -\beta^i_k\varepsilon^i_k\frac{r^i_k}{\rho^i_k}$ rise to levels that trigger the input saturation, i.e., $\text{sat}\,(u^i_k) - u^i_k \neq 0$. The non-negative second term in (11) is activated to compensate for the exponential decrease of the boundary caused by the first term for all $t > 0$, confining the combined errors within the boundaries. Despite the large s_k^i, the relaxation of ρ_k^i causes the normalized errors $\xi_{sk}^i = \frac{s_k^i}{\rho_k^i}$ to decrease, which in turn leads to lower transformed errors ε_k^i and r_k^i. As a result, the input signals u_k^i decrease, deactivating the input saturation due to the relaxation of ρ_k^i.

- Unsaturated inputs case: when the combined errors s_k^i are small and far away from the boundary of the envelope, the normalized errors $\xi_{sk}^i = \frac{s_k^i}{\rho_k^i}$ are also small. This results in small transformed errors ε_k^i and r_k^i. In this scenario, the input signals u_k^i are too small to trigger the input saturation , i.e. $\text{sat}\,(u_k^i) - u_k^i = 0$, so the second term is not activated. Here, the first term in (11) represents the conventional performance function (10). It is important to note that if $\xi_{sk}^i = 0$, then $\varepsilon_k^i = 0$, consequently $u_k^i = 0$, and there is no chance for the zero input to be saturated, thus, the second term would not be activated.

Therefore, the adaptive prescribed performance function in (11) relaxes when the input saturation occurs and recovers to the conventional prescribed performance function as in (10) when the input saturation vanishes. The above analysis illustrates how our adaptive framework effectively dampens the input saturation without the need for an auxiliary system. Accordingly, the adaptive performance function ρ_k^i in (11) is always positive for all $t > 0$, $k = 1, \ldots, n$, $i = 1, \ldots, N$.

Remark 2. *It is worth noting that when the saturation levels $\bar{u}_k^i$ in (2) are sufficiently large, the second term in (11) is relatively small compared with the first term, leading to an overall decreasing effect on the performance function ρ_k^i when it reaches certain values $\bar{\rho}_k^i \in \mathbb{R}^+$. Thus, there exist positive constants $\bar{\rho}_k^i$ such that the prescribed performance functions $\rho_k^i \in (0, \bar{\rho}_k^i]$ given sufficiently large saturation levels $\bar{u}_k^i$ for $k = 1, \ldots, n$ and $i = 1, \ldots, N$ [29].*

Theorem 1. *Consider a leader agent with trajectory represented by $q^0(t)$ and multiple follower agents modeled by (1) with an augmented communication graph $\bar{\mathcal{G}} = (\bar{\mathcal{V}}, \bar{\mathcal{E}})$ that satisfies Assumption 1. For sufficiently large saturation levels $\bar{u}_k^i$, there exist upper bounds $\bar{\rho}_k^i$ of the performance functions $\rho_k^i(t)$ in (11) such that the closed-loop system (1) under the control (9) fulfills:*

$$-\bar{\rho}_k^i \le -\rho_k^i(t) < s_k^i < \rho_k^i(t) \le \bar{\rho}_k^i, \qquad \forall t \ge 0 \tag{12}$$

for $k = 1, \ldots, n$ and $i = 1, \ldots, N$.

Remark 3. *Notably, the controller design in this work uses only local information from the neighbors without requiring any global information (such as the topology structure). In addition, no approximation structures for the uncertainties in the dynamics are employed.*

Remark 4. *On one hand, communication topology only describes the interaction caused by the control protocol via sensor communication (i.e. the state error $e_k^i, \dot{e}_k^i$ between multiple agents in (3) is required for the control design $u_k^i = -\beta_k^i \frac{r_k^i \varepsilon_k^i}{\rho_k^i}$ in (9)). On the other hand, the physical interconnection terms $H^i(q^i, q^j, \dot{q}^i, \dot{q}^j)$ exist intrinsically in the dynamics, which is a part of the system dynamics before the control protocol is applied. Therefore, physical interconnection not caused by the control protocol has a direct effect on the dynamics, which should not be ignored.*

IV. Stability Analysis

The proof of Theorem 1 proceeds as follows.

Proof. Let us define the vectors of normalized tracking errors

$$\xi_s^i = [\xi_{s1}^i, \ldots, \xi_{sn}^i]^T = [\frac{s_1^i}{\rho_1^i}, \ldots, \frac{s_n^i}{\rho_n}]^T = (\rho^i)^{-1} s^i \tag{13}$$

where $\rho^i = \text{diag}([\rho_1^i, \ldots, \rho_n^i])$ and $s^i = [s_1^i, \ldots, s_n^i]^T$ for $i = 1, \ldots, N$. Therefore, we have the compact form of (13) as

$$\xi_s = \rho^{-1} s \tag{14}$$

with $\rho = \text{diag}([\rho^1, \ldots, \rho^N]), s = [s^1, \ldots, s^N]^T$.

Differentiating (14) with respect to time, we obtain

$$\dot{\xi}_s = \rho^{-1}(\dot{s} - \dot{\rho}\xi_s). \tag{15}$$

with $\dot{\rho} = \text{diag}([\dot{\rho}^1, \ldots, \dot{\rho}^N]), \dot{\rho}^i = \text{diag}([\dot{\rho}_1^i, \ldots, \dot{\rho}_n^i])$.

Thus, the compact form of the dynamics in (1) can be written as

$$\ddot{q} = M^{-1}[\tau - C\dot{q} - (\Theta \otimes I_n)q - G - F - H - d] \tag{16}$$

with $q = [q^1, \ldots, q^N]^T$, $M = \text{diag}([M^1, \ldots, M^N])$, $C = \text{diag}([C_1, \ldots, C_N])$, $G = [G_1, \ldots, G_N]$, $F = [F_1, \ldots, F_N]$, $H = [H_1, \ldots, H_N]$, $d = [d^1, \ldots, d^N]^T$, $d^i = [d_1^i, \ldots, d_n^i]^T$, $\tau = [\tau^1, \ldots, \tau^N]^T$, $\tau^i = [\tau_1^i, \ldots, \tau_n^i]^T$ for $i = 1, \ldots, N$.

Moreover, the vector of input in (9) can be written as

$$u(t) = -\beta r \rho^{-1} \varepsilon \tag{17}$$

where $u = [u^1, \ldots, u^N]^T$, $\beta = \text{diag}([\beta^1, \ldots, \beta^N])$, $r = \text{diag}([r^1, \ldots, r^N])$, $\varepsilon = [\varepsilon^1, \ldots, \varepsilon^N]^T$ with $u^i = [u_1^i, \ldots, u_n^i]^T$, $\beta^i = \text{diag}([\beta_1^i, \ldots, \beta_n^i])$, $r^i = \text{diag}([r_1^i, \ldots, r_n^i])$, $\varepsilon^i = [\varepsilon_1^i, \ldots, \varepsilon_n^i]^T$. Here $\beta_k^i > 0$ are user-defined constants, $i = 1, \ldots, N$, $k = 1, \ldots, n$.

Combining (5) and (6), the vector of combined errors are obtained as

$$s = \dot{e} + Pe = \big((\mathcal{L} + B) \otimes I_n\big)(\dot{\delta} + P\delta) \tag{18}$$

with $s = [s^1, \ldots, s^N]^T, s^i = [s_1^i, \ldots, s_n^i]^T, P = \text{diag}([\alpha, \ldots, \alpha])$.

Differentiating (18) with respect to time and substituting (16), we get

$$\begin{aligned}\dot{s} =& \big((\mathcal{L} + B) \otimes I_n\big)(\ddot{\delta} + P\dot{\delta}) = \big((\mathcal{L} + B) \otimes I_n\big)(\ddot{q} - \ddot{\underline{q}}^0 \\ & + \alpha\dot{q} - \alpha\dot{\underline{q}}^0) \\ =& \big((\mathcal{L} + B) \otimes I_n\big)\big\{M^{-1}[\tau - C\dot{q} - G - F - H - d] \\ & - \ddot{\underline{q}}^0 + \alpha q - \alpha\dot{\underline{q}}^0\big\}\end{aligned} \tag{19}$$

Define $\xi = [q^T\ \dot{q}^T\ \xi_s^T]^T \in \mathbb{R}^{3nN}$. Differentiating ξ, and substituting (2), (17), (19) into (15), we have closed-loop dynamical system of ξ

$$\begin{aligned}\dot{\xi} =&\rho^{-1}\Big\{\big((\mathcal{L}+B)\otimes I_n\big)\big\{M^{-1}[-\operatorname{sat}(\beta r\rho^{-1}\varepsilon)-C\dot{q}\\&-G-F-H-d]-\underline{\ddot{q}}^0+\alpha q-\alpha\underline{\dot{q}}^0\big\}\\&+\lambda(\rho-\rho_\infty)\xi+\gamma[\operatorname{sat}(\beta r\rho^{-1}\varepsilon)-\beta r\rho^{-1}\varepsilon]\Big\}\\&=\varphi(t,\xi)\end{aligned}\tag{20}$$

where $\rho_\infty = \operatorname{diag}([\rho_\infty^1,\ldots,\rho_\infty^N])$, $\rho_\infty^i = \operatorname{diag}([\rho_1^i(\infty),\ldots,\rho_n^i(\infty)])$, $\lambda = \operatorname{diag}([\lambda^1,\ldots,\lambda^N])$, $\lambda^i = \operatorname{diag}([\lambda_1^i,\ldots,\lambda_n^i])$, $\beta r\rho^{-1}\varepsilon = [\beta^1 r^1(\rho^1)^{-1}\varepsilon^1,\ldots,\beta^N r^N(\rho^N)^{-1}\varepsilon^N]^T$, $\operatorname{sat}(\beta r\rho^{-1}\varepsilon) = [\operatorname{sat}(\beta^1 r^1(\rho^1)^{-1}\varepsilon^1),\ldots,\operatorname{sat}(\beta^N r^N(\rho^N)^{-1}\varepsilon^N)]^T$, $\gamma = \operatorname{diag}([\gamma^1,\ldots,\gamma^N])$, $\beta^i r^i {\rho^i}^{-1}\varepsilon^i = [\frac{\beta_1^i r_1^i\varepsilon_1^i}{\rho_1^i},\ldots,\frac{\beta_n^i r_n^i\varepsilon_n^i}{\rho_n^i}]^T$, $\operatorname{sat}(\beta^i r^i(\rho^i)^{-1}\varepsilon^i) = [\operatorname{sat}(\frac{\beta_1^i r_1^i\varepsilon_1^i}{\rho_1^i}),\ldots,\operatorname{sat}(\frac{\beta_n^i r_n^i\varepsilon_n^i}{\rho_n^i})]^T$, $\gamma^i = \operatorname{diag}([\gamma_1^i,\ldots,\gamma_n^i])$ for $i=1,\ldots,N$.

Define open sets $\Omega \subset \mathbb{R}^{3nN}$, $\Omega_q \subset \mathbb{R}^{nN}$, $\Omega_{\dot{q}} \subset \mathbb{R}^{nN}$, $\Omega_s \subset \mathbb{R}^{nN}$ with $\Omega = \Omega_q\times\Omega_{\dot{q}}\times\underbrace{[-1,1]\times\ldots\times[-1,1]}_{\Omega_s}$ where $\Omega_q,\Omega_{\dot{q}}$ are constant sets defined by user.

Subsequently, provided a sufficiently large saturation level of the input signal, three steps are followed: Step A guarantees the existence of a unique maximal solution for ξ in (20) such that $\xi(t):[0,T_{\max}]\to\Omega$, i.e. $\xi(t)\in\Omega$, $\forall t\in[0,T_{\max}]$. Then, in Step B, the proposed distributed controllers in (9) and the adaptive performance functions in (11) are proved to guarantee $\forall t\in[0,T_{\max}]$ the boundedness of closed-loop signals. We also explore conditions on the saturation level $\bar{u}_k^i$ in (2) that guarantees the boundedness of ρ_k^i. In Step C, $\xi(t)$ is shown to remain strictly within a compact subset of Ω, resulting in $T_{\max}=\infty$ by contradiction.

Step A: Unique maximum solution $\boldsymbol{\xi(t)}$ of (20). It holds that $\xi_s(0)\in\Omega_s$ by selecting appropriate $\rho_k^i(0) > |s_k^i(0)|$ leading to $|\xi_{sk}^i(0)| = |s_k^i(0))/\rho_k^i(0)| < 1$, $k=1,\ldots,n$, $i=1,\ldots,N$. Although the exact bounds Ω_q and $\Omega_{\dot{q}}$ are unknown, both $q(0)$ and $\dot{q}(0)$ are finite constant vectors that are bounded, depending on our selection of initial states. This implies that there exist sets Ω_q and $\Omega_{\dot{q}}$ from which we can choose suitable $q(0)$ and $\dot{q}(0)$ to ensure $q(0)\in\Omega_q$ and $\dot{q}(0)\in\Omega_{\dot{q}}$. Consequently, we will have $\xi(0) = [q^T(0)\ \dot{q}^T(0)\ \xi_s^T(0)]^T\in\Omega$. Due to the continuity and locally integrability on $q(t),\dot{q}(t)$ of unknown nonlinearities $M(q),C(q,\dot{q}),G(q),F(\dot{q}),H(q,\dot{q})$, $\forall t\in[0,T_{\max}]$, the piecewise continuity and integrability of $d(t),\underline{\dot{q}}^0,\underline{\ddot{q}}^0$ for $t\ge 0$, as well as the boundedness of ρ due to $\rho_k^i\in(0,\bar{\rho}]$ under sufficiently large saturation levels u_k^i, as well as the piecewise continuity of controller input $u(t)$ and saturation of the controller $\tau=\operatorname{sat}(u)$ on t, the right-hand side $\varphi(t,\xi)$ in (20) is a piecewise continuous on t and locally Lipschitz on ξ over the set Ω. Therefore, the hypotheses of Initial Value Theorem [39, Th. 54, pp. 476] hold, ensuring thus the existence of a maximal solution $\xi(t)$ of (20) on a time interval $[0,T_{\max}]$ such that $\xi(t) = [q^T(t)\ \dot{q}^T(t)\ \xi_s^T(t)]^T\in\Omega,\forall t\in[0,T_{\max}]$. As a result, we have $\xi_s(t)\in\Omega_s, q(t)\in\Omega_q,\dot{q}(t)\in\Omega_{\dot{q}}\ \forall t\in[0,T_{\max}]$. Thus, all $\xi_s(t),q(t),\dot{q}(t)$ are proven to be bounded for all $t\in[0,T_{\max}]$.

Step B: Proof the boundedness of all closed-loop signals, $\boldsymbol{\forall t\in[0,T_{\max}]}$. Consider a positive definite Lyapunov function

$$V=\frac{1}{2}\varepsilon^T\varepsilon\tag{21}$$

Differentiating (21) and substituting (20), we have

$$\begin{aligned}\dot{V} &= \varepsilon^T\rho^{-1}r\Big\{\big((\mathcal{L}+B)\otimes I_n\big)\big\{M^{-1}[-sat(\beta r\rho^{-1}\varepsilon)-C\dot{q}\\&-G-F-H-d]-\underline{\ddot{q}}^0+\alpha q-\alpha\underline{\dot{q}}^0\big\}\\&+\lambda(\rho-\rho_\infty)\xi_s+\gamma[sat(\beta r\rho^{-1}\varepsilon)-\beta r\rho^{-1}\varepsilon]\Big\}\\&=\varepsilon^T\rho^{-1}r\big[-\gamma\beta r\rho^{-1}\varepsilon+Z_1(q,\dot{q})+Z_2(q)\operatorname{sat}(\beta r\rho^{-1}\varepsilon)\big]\end{aligned}\tag{22}$$

where

$$\begin{aligned}Z_1(q,\dot{q}) =& -\big((\mathcal{L}+B)\otimes I_n\big)\big\{M^{-1}[C\dot{q}+G+F+H+d]\\&+\underline{\ddot{q}}^0+\alpha\underline{\dot{q}}^0-\alpha q\big\}+\lambda(\rho-\rho(\infty))\xi_s\\Z_2(q) =& \gamma-\big((\mathcal{L}+B)\otimes I_n\big)M^{-1}\end{aligned}$$

where $\rho_k^i\in(0,\bar{\rho}]$ for all $t\ge 0$ under sufficiently large saturation levels $\bar{u}_k^i$. In Step A, it has been concluded that $\xi_s\in\Omega_s, q(t)\in\Omega_q,\ \dot{q}(t)\in\Omega_{\dot{q}}\ \forall t\in[0,T_{\max}]$. In addition, the uncertain nonlinearities $M(q),G(q,\dot{q}),C(q),F(\dot{q}),H(q,\dot{q})$ are continuous functions on $q(t)$ and $\dot{q}(t)$ for $t\in[0,T_{\max}]$. That is, these continuous nonlinearities explicitly depend on time t. By applying the Extreme Value Theorem to these nonlinearities $M(q),G(q,\dot{q}),C(q),F(\dot{q}),H(q,\dot{q})$, their boundedness is ensured over the closed time interval $t\in[0,T_{\max}]$. Combining the above analysis with the boundedness of $d(t),\underline{\dot{q}}^0,\underline{\ddot{q}}^0\ \forall t\ge 0$ by assumption, there exists a positive upper bound $\bar{Z}$ (a constant independent of $T_{\max}$) such that

$$\bar{Z}=\sup_{\rho\le\bar{\rho}}\Big\|Z_1(q,\dot{q})+Z_2(q)\operatorname{sat}(\beta r\rho^{-1}\varepsilon)\Big\|.\tag{23}$$

From the definition of $r_k^i = \frac{1}{(1-\xi_{sk}^i)(1+\xi_{sk}^i)}$, the minimum eigenvalue of r satisfies $\underline{\sigma}(r)\ge 1$. Due to the symmetric property of diagonal matrices γ, β, and substituting (23) into (22), we have

$$\begin{aligned}\dot{V} &\le -\varepsilon^T\rho^{-1}r\gamma\beta r\rho^{-1}\varepsilon+\bar{Z}\|\rho^{-1}r\varepsilon\|\\&\le -\frac{1}{2}\underline{\sigma}(\gamma\beta)\underline{\sigma}^2(\rho^{-1})\|\varepsilon\|^2-\frac{1}{2}\underline{\sigma}(\gamma\beta)\|\varepsilon^T\rho^{-1}r\|^2+\bar{Z}\|\rho^{-1}r\varepsilon\|\\&\le -\frac{1}{2}\underline{\sigma}(\gamma\beta)\underline{\sigma}^2(\rho^{-1})\|\varepsilon\|^2+\frac{\bar{Z}^2}{2\underline{\sigma}(\gamma\beta)}\end{aligned}\tag{24}$$

where $\underline{\sigma}(\gamma\beta)$, $\underline{\sigma}(\rho^{-1})$ denote the minimum singular value of $\gamma\beta$ and ρ^{-1}, respectively. It is concluded that $\dot{V}\le 0$ when $\|\varepsilon\|\ge\frac{\bar{Z}}{\underline{\sigma}(\gamma\beta)\underline{\sigma}(\rho^{-1})}$. Consequently, we have

$$\|\varepsilon\|\le\bar{\varepsilon}=\max\Big\{\varepsilon(0),\frac{\bar{Z}}{\underline{\sigma}(\gamma\beta)\underline{\sigma}(\rho^{-1})}\Big\}\tag{25}$$

When the performance functions ρ_k^i reach the upper bounds $\bar{\rho}_k^i$, $k=1,\ldots,n$, $i=1,\ldots,N$, a sufficient condition to guarantee the stability of the closed-loop system (20) is that the right-hand side of (11) be negative with sufficiently large input saturation levels $\bar{u}_k^i$, i.e.,

$$\lambda_k^i(\bar{\rho}_k^i-\rho_k^i(\infty))\ge\gamma_k^i\frac{\operatorname{sat}(\frac{\beta_k^i r_k^i\varepsilon(\bar{\rho}_k^i)}{\bar{\rho}_k^i})-\frac{\beta_k^i r_k^i\varepsilon(\bar{\rho}_k^i)}{\bar{\rho}_k^i}}{\xi_s(\bar{\rho}_k^i)}\ge 0\tag{26}$$

where $\xi_s(\bar{\rho}_k^i) = s_k^i/\bar{\rho}_k^i$, $\varepsilon_{\bar{\rho}_k^i} = \ln\left[\left(1+\xi_{\bar{\rho}_{sk}^i}\right)/\left(1-\xi_{\bar{\rho}_{sk}^i}\right)\right]$. Since $-\bar{u}_k^i \leq \mathrm{sat}(\frac{\beta_k^i r_k^i \varepsilon_{\bar{\rho}_k^i}}{\bar{\rho}_k^i}) \leq \bar{u}_k^i$, from (26) it is concluded that there exist upper bounds $\bar{\rho}_k^i > 0$ such that $\rho_k^i \in (0, \bar{\rho}_k^i]$ when the saturation level $\bar{u}_k^i$ satisfies

$$\begin{aligned}\bar{u}_k^i > \max\Big\{&\beta_k^i r_k^i \bar{\rho}_k^{i\,-1}\varepsilon_{\bar{\rho}_k^i} + \frac{1}{\gamma_k^i}\lambda_k^i(\bar{\rho}_k^i - \rho_k^i(\infty))\xi_s(\bar{\rho}_k^i),\\ &-\beta_k^i r_k^i \bar{\rho}_k^{i\,-1}\varepsilon_{\bar{\rho}_k^i} - \frac{1}{\gamma_k^i}\lambda_k^i(\bar{\rho}_k^i - \rho_k^i(\infty))\xi_s(\bar{\rho}_k^i)\Big\} \end{aligned} \quad (27)$$

for $i = 1, \ldots, N,\ k = 1, \ldots, n$. Owing to the continuity of r_k^i, ρ_k^i, ε_k^i and ξ_{sk}^i, the right-hand side of inequality (27) is bounded. As a result, all signals of the closed-loop system in (20) are bounded for sufficiently large saturation levels $\bar{u}_k^i$ that satisfy (27). Thus, the stability of the system is guaranteed for all $t \in [0, T_{\max}]$. Taking the inverse of the logarithmic function, and combining with (25), we get a hyperbolic tangent function satisfying

$$-1 < \tanh(-\bar{\varepsilon}) = \underline{\xi}_s \leq \xi_{sk}^i \leq \bar{\xi}_s = \tanh(\bar{\varepsilon}) < 1 \quad (28)$$

for $i = 1, \ldots, N$, and $k = 1, \ldots, n,\ \forall t \in [0, T_{\max}]$. Hence it is implied from (28) that the normalized error $\xi_s(t)$ remains bounded with a nonempty compact set $\Omega^{'}$ with

$$\Omega_s^{'} := [\underline{\xi}_s, \bar{\xi}_s] \times \ldots \times [\underline{\xi}_s, \bar{\xi}_s] \subset \Omega_s \in \mathcal{R}^{nN}, \forall t \in [0, T_{\max}] \quad (29)$$

Furthermore, the boundedness of ξ_{sk}^i implies the boundedness of s_k^i within the prescribed performance bounds as in (12) for $i = 1, \ldots, N$, and $k = 1, \ldots, n$. The combined error s is defined as a stable filter, satisfying the bounded-input, bounded-output (BIBO) property that ensures the boundedness of $e, \dot{e}$ when s is bounded for all $t \in [0, T_{\max}]$.

Step C: Prove that $T_{\max}$ can be extended to ∞. According to (29) , it is indicated that $\xi_s(t) \in \Omega_s^{'} \subset \Omega_s, \forall t \in [0, T_{\max}]$ since $[\underline{\xi}_s, \bar{\xi}_s] \subset (-1, 1)$. Hence, assuming that $T_{\max} < \infty$, then according to [39, Prop.C.3.6, pp.481] there exists a time instant $t^{'} \in [0, T_{\max}]$ such that $\xi_s(t^{'}) \notin \Omega_s^{'}$, which is contradiction. Consequently, this assumption is untenable, i.e. $T_{\max} = \infty$ with $t \in [0, T_{\max}]$ such that $\xi_s(t) \in \Omega_s^{'} \subset \Omega_s$. Consequently, all closed-loop signals of (20) remain bounded $\forall t \geq 0$. Combining (14) with (28), we arrive at

$$-\bar{\rho}_k^i \leq -\rho_k^i(t) < s_k^i < \rho_k^i(t) \leq \bar{\rho}_k^i, \qquad \forall t \geq 0$$

□

Remark 5. *The Euler-Lagrange system we are considering is subject to structural uncertainties (i.e., $M(q), C(q, \dot{q}), G(q), F(\dot{q}), H(q, \dot{q})$) in eq(1), resulting in uncertain terms (such as Z_1, Z_2 in (23)) in Lyapunov analysis. This makes it challenging to determine their exact values in practice. Therefore, it is quite difficult to establish precise conditions for the saturation levels instead of inequality (27).*

Remark 6. *The phrase "sufficiently large", employed to characterize the input saturation levels $\bar{u}_k^i$, serves as a qualitative description rather than an absolute measurement. Therefore, the actual values of input saturation levels $\bar{u}_k^i$ depend on the specific systems, including structures and parameters of the systematic nonlinearities ($M^i(q^i)$, $C^i(q^i, \dot{q}^i)$, $G^i(q)$, $F(\dot{q})$, $H^i(q^i, q^j, \dot{q}^i, \dot{q}^j)$), as well as the selection of prescribed performance function ρ_k^i, which includes the decreasing rate λ_k^i, initial value $\rho_k^i(0)$, and final value $\rho_k^i(\infty)$, the coefficient γ_k^i.*

Remark 7. *It is important to choose the parameters of the adaptive prescribed performance function ρ_k^i in Eq. (12) carefully and tune the control gains of u_k^i in Eq. (11) appropriately to ensure that Eq. (13) holds. In particular, the selection of the performance parameters of ρ_k^i and tuning control gains of u_k^i should adhere to the following principles:*
1) The initial conditions must satisfy $\rho_k^i(0) \geq \rho_k^i(\infty) > 0$, $\rho_k^i(0) > |s_k^i(\tilde{e}_k^i(0))|$;
2) The evolution of ρ_k^i is coupled with the control gains β_k^i, α_k^i and performance parameters λ_k^i, γ_k^i. A larger β_k^i leads to a faster saturation of the control signal u_k^i according to Eq. (11). And an increase in α_k^i causes the combined error to increase, making it possible to reach or even cross the boundaries of the envelope. Furthermore, increasing γ_k^i leads to greater relaxation of ρ_k^i when the input saturation is activated, as indicated by the second term in Eq. (12), leading to an increase in the envelope bound. As λ_k^i increases, ρ_k^i decreases faster, and it becomes possible for the combined error to cross the envelope bound, potentially resulting in system instability. Therefore, the selection of PPC parameters and control gains is primarily based on the ratio $\frac{\lambda_k^i \alpha_k^i}{\beta_k^i \gamma_k^i}$, which should be relatively small.

Remark 8. *The above analysis reveals that the distributed controllers and adaptive prescribed performance functions are effective in confining the combined errors despite in the presence of input saturation. The analysis indicates that the influence caused by physical interconnection terms, unknown nonlinearities, and external disturbances can effectively be compensated.*

V. Simulation Results

A. Generic Evaluation

We will consider six interconnected EL systems (cf. Fig. 1), representing two-link robot arms with equations of motion as:

$$\begin{aligned}&\begin{bmatrix} M_{11}^i & M_{12}^i \\ M_{12}^i & M_{22}^i \end{bmatrix}\begin{bmatrix} \ddot{q}_1^i \\ \ddot{q}_2^i \end{bmatrix} + \begin{bmatrix} c_i\dot{q}_2^i & c_i(\dot{q}_1^i + \dot{q}_2^i) \\ -c_i\dot{q}_1^i & 0 \end{bmatrix}\begin{bmatrix} \dot{q}_1^i \\ \dot{q}_2^i \end{bmatrix}\\ &+ \begin{bmatrix} H_1^i \\ H_2^i \end{bmatrix} + \begin{bmatrix} G_1^i \\ G_2^i \end{bmatrix} + \begin{bmatrix} F_1^i \\ F_2^i \end{bmatrix} + \begin{bmatrix} d_1^i \\ d_2^i \end{bmatrix} = \begin{bmatrix} \tau_1^i \\ \tau_2^i \end{bmatrix} \end{aligned} \quad (30)$$

where

$$\begin{aligned}&M_{11}^i = (m_1^i + m_2^i)r_1^2 + m_2^i r_2^2 + 2m_2^i r_1 r_2 \cos(q_2^i) + J_1,\\ &M_{12}^i = m_2^i r_2^2 + m_2^i r_1 r_2 \cos(q_2^i),\ M_{22}^i = m_2^i r_2^2 + J_2,\\ &G_1^i = (m_1^i + m_2^i) r_1 g \cos(q_1^i) + m_2^i r_2 g \cos(q_1^i + q_2^i),\\ &G_1^i = m_2^i r_2 g \cos(q_1^i + q_2^i),\ c_i = -m_2^i r_1 r_2 \sin(q_2^i)\\ &F_1^i(\dot{q}_1^i) = f_1^i \tanh(f_2^i\dot{q}_1^i) - \tanh(f_3^i\dot{q}_1^i)) + f_4^i \tanh(f_5^i\dot{q}_1^i) + f_6^i\dot{q}_1^i\\ &F_2^i(\dot{q}_2^i) = f_1^i \tanh(f_2^i\dot{q}_2^i) - \tanh(f_3^i\dot{q}_2^i)) + f_4^i \tanh(f_5^i\dot{q}_2^i) + f_6^i\dot{q}_2^i\end{aligned}$$

To enhance the system heterogeneity, six dynamics's unknown parameters are compactly represented as $\Theta_i = [m_1^i \; m_2^i \; f_1^i \; f_2^i \; f_3^i \; f_4^i \; f_{i5}^i \; f_{i6}]^T$ with

$$\Theta_1 = [0.6 \; 1.2 \; 0.5 \; 0.8 \; 0.9 \; 1.2 \; 0.5 \; 0.4]^T$$
$$\Theta_2 = [0.8 \; 1.2 \; 0.5 \; 0.7 \; 0.9 \; 1.0 \; 0.5 \; 0.4]^T$$
$$\Theta_3 = [0.9 \; 1.3 \; 0.3 \; 0.7 \; 0.7 \; 1.0 \; 0.7 \; 0.3]^T$$
$$\Theta_4 = [0.5 \; 1.4 \; 0.5 \; 0.9 \; 0.7 \; 1.2 \; 0.4 \; 0.5]^T$$
$$\Theta_5 = [0.7 \; 1.2 \; 0.5 \; 0.8 \; 0.6 \; 1.3 \; 0.5 \; 0.6]^T$$
$$\Theta_6 = [0.4 \; 1.4 \; 0.6 \; 1.0 \; 0.9 \; 1.5 \; 0.2 \; 0.5]^T$$

The friction term F_i is taken in non-linear-in-the-parameters form according to [40]. The values of the systematic parameters are selected as $r_1 = 1.0, r_2 = 0.8, J_1 = 5, J_2 = 5$. Inspired by the viscoelasticity model in [41], the physical interconnection term is given in the form of springs-dampers: $H^i(q^i, q^j, \dot{q}^i, \dot{q}^j) = \sum_{j \in \mathcal{N}_i'} \theta_{ij}(q^i - q^j) + \upsilon_{ij}(\dot{q}^i - \dot{q}^j)$ where $\theta_{ij} > 0$ and $\upsilon_{ij} > 0$, $i = 1, \ldots, 6$, $j = 1, \ldots, 6$ are the stiffness parameters and the damping factors on the edge $(v_i, v_j) \in \mathcal{E}'$, respectively. Based on the physical interconnection network in Fig. 1, the spring-damper parameters are chosen as $\theta_{12} = \theta_{21} = 0.21$, $\theta_{46} = \theta_{64} = 0.29$ and $\nu_{12} = \nu_{21} = 2$, $\theta_{46} = \nu_{64} = 1$ for interconnection 1 (cf. Fig. 1a), and $\theta_{52} = \theta_{25} = 0.37$, $\theta_{36} = \theta_{63} = 0.25$, and $\theta_{52} = \theta_{25} = 5$, $\theta_{36} = \theta_{63} = 1$ for interconnection 2 (cf. Fig. 1b). (all these values are used for simulation but are unknown for control design).

The leader's trajectory is chosen as $q_1^0 = 1.25 - (7/5)\exp^{-t} + (7/20)\exp^{-4t}$, $q_2^0 = 1.25 + \exp^{-t} - (1/4)\exp^{-t}$. We select the external disturbance as $d_i(t) = 4\cos(t)[1 \;\; 1]^T$. The initial values of state variables are chosen as $q^i(0) = [\sin(i/3) \quad 1.5\cos(i/3)]^T$ for $i = 1, \ldots, N$. The values of performance and control parameters are listed in Tables I and II. Specifically, the initial values of $\rho_k^i(t)$ are chosen to satisfy the condition $\rho_k^i(0) > |s_k^i(0)|$ for $i = 1, \ldots, N, k = 1, 2$.

Table I: Performance parameters

$\rho_k^i(0)$	$\rho_k^i(\infty)$	λ_k^i	γ_k^i	$\bar{u}^i$
$2\|s_k^i(0)\| + 1$	0.001	0.5	0.5	$[30 \; 12]^T$

Table II: Control parameters in the proposed control

α	β_k^i
1	1

The simulation results for interconnection 1 are presented in Fig. 2. In Fig. 2a, we can observe that the combined errors s_k^i evolve within the adaptive prescribed performance functions ρ_k^i with the input constraints for six follower agents under physical Interconnection 1. The prescribed boundaries are relaxed when the input saturation reaches certain levels, resulting in different extensions of the boundaries for varying levels of saturation. Fig. 2b shows that the actual saturated inputs τ_k^i, which are less than or equal to the desired inputs u_k^i, are constrained to the intervals $[-\bar{u}_k^i, \bar{u}_k^i]$ due to input saturation in (2) for $i = 1, \ldots, N$, $k = 1, \ldots, n$.

B. Sensitivity analysis

Without loss of generality, we also test different physical interconnection structures, i.e., Interconnection 2, by using the same parameters as Interconnection 1. The simulation results for interconnection 2 are shown in Fig. 3, where the adaptive prescribed boundaries ρ_k^i also effectively restrain the combined errors s_k^i under the input constraints. Table III shows minor differences in terms of combined error and input norms for Interconnection 1 and Interconnection 2 in the proposed control scheme. These results demonstrate that the proposed approach can accommodate different structures of physical interconnections.

Table III: L_2 norms of combined error and input for different interconnection structures in the proposed control

Interconnection structure	Error norm	Input norm
Interconnection1	6.33	2.70×10^3
Interconnection2	6.33	2.52×10^3

We then conduct a sensitivity analysis with different disturbances d_i for Interconnection 1, i.e. cosine disturbances with different frequencies. Adjusting to different disturbances requires the use of different control parameters and saturation levels, which involves a tedious trial-and-error process of parameter selection. Table IV shows the same error norm with slight variations in input norms for different disturbances, which validates the robustness of the proposed control scheme.

Table IV: L_2 norms of combined error and input for different disturbances in the proposed control

Disturbance	Error norm	Input norm
$d_i = 4\cos(t)[1 \; 1]^T$	6.33	2.70×10^3
$d_i = 4\cos(0.001t)[1 \; 1]^T$	6.33	2.84×10^3
$d_i = 4\cos(10t)[1 \; 1]^T$	6.33	2.91×10^3

C. Comparative Study

To validate the proposed distributed controllers in (9) and adaptive prescribed performance functions in (11), we consider the adaptive sliding mode control scheme in [31] to compare with because both [31] and our work focus on the uncertain Euler-Lagrange system with input constraints using an adaptive approach. However, [31] does not consider prescribed performance control, whereas our work incorporates it. Therefore, we compare our results with those of [31] to highlight the differences in the response of input-constrained Euler-Lagrange systems when applying prescribed performance control versus not applying it. In order to make a proper comparison, we extend [31] from centralized to distributed control, while the initial condition and some parameters are the same as in Sect V. A.

The simulation results of [31] in Fig. 4 are tuned to get the best performance. The values of the control parameters are shown in Table V, where five control parameters need to be tuned in [31]. However, it can be observed from Table II that only two control parameters need to be tuned in our work, particularly when the parameter α is uniform across all agents. The number of control parameters we need to tune is significantly lower than in most PPC papers, emphasizing the low complexity of our approach.

Table V: Control parameters in [31]

c^i_{1k}	c^i_{2k}	μ^i_k	ψ^i_k	α^i_k
0.5	0.5	1	20	10

Table VI: L_2 norm of combined error and input for different interconnection structures in [31]

Interconnection structure	Error norm	Input norm
Interconnection 1	507.87	3.19×10^3
Interconnection 2	566.70	3.29×10^3

One can observe from Fig. 4a that the steady-state responses do not consistently remain within the proposed boundaries for most agents. Additionally, even when some steady-state responses do fall within the boundaries, the transient-state responses for certain agents cross the proposed boundaries. This observation is further supported by the comparison between Fig. 2c and Fig. 4c, where the normalized errors ξ^i_{sk} remain within the interval $[-1,\ 1]$ in our work while ξ^i_{sk} oscillate dramatically (the maximum intervals can be $[-1500, 0]$) in the adaptive sliding mode control [31] for Interconnection 1. The analysis is also applicable to Interconnection 2. Due to the space limit, we omit the figure of Interconnection 2.

In addition, when comparing Table III and Table VI, it is evident that the combined error norms are much bigger, even with larger input norms both for Interconnection 1 and Interconnection 2 in the adaptive sliding mode control [31] compared to the proposed control scheme.

VI. Conclusions

A distributed control protocol for uncertain interconnected Euler-Lagrange systems constrained by input saturation is proposed. Adaptive performance functions are introduced, which can flexibly adjust the boundary envelope based on the activation of input saturation without the need for an auxiliary system. Prescribed transient and steady-state performance on a combined error under amplitude input saturation is achieved. In addition, intrinsic couplings due to physical interconnection are considered. Finally, the structural uncertainties in dynamics are tackled without approximation. Based on this paper, our future work will focus on addressing the formation control of multi-agent systems and dynamically changing topologies.

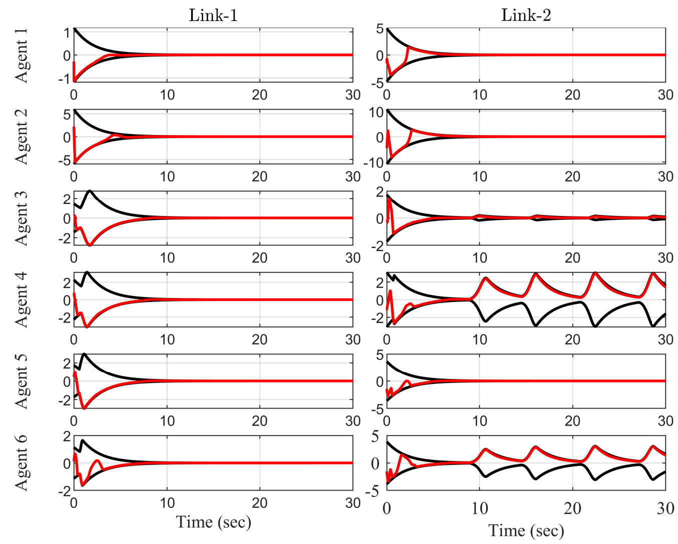

(a) Combined errors s^i_k (black lines: $\pm\rho^i_k(t)$, red lines: s^i_k)

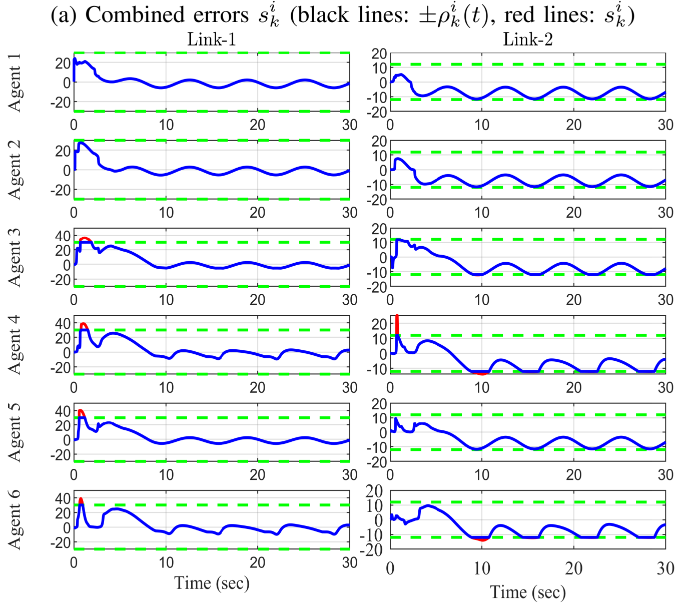

(b) Input signals (red solid line: u^i_k, blue solid lines: τ^i_k, green dotted lines: $\pm\bar{u}^i_k$)

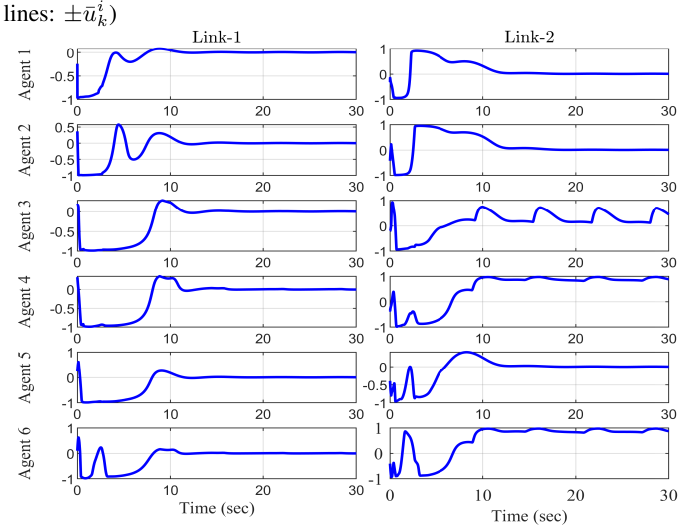

(c) Normalized errors ξ^i_{sk}

Figure 2: System performance of Interconnection 1 for the proposed control.

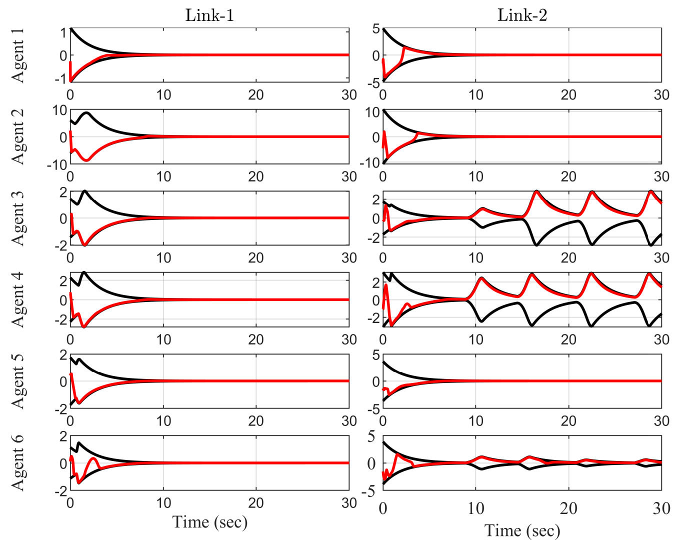

(a) Combined errors s_k^i(black lines: $\pm\rho_k^i(t)$, red lines: s_k^i)

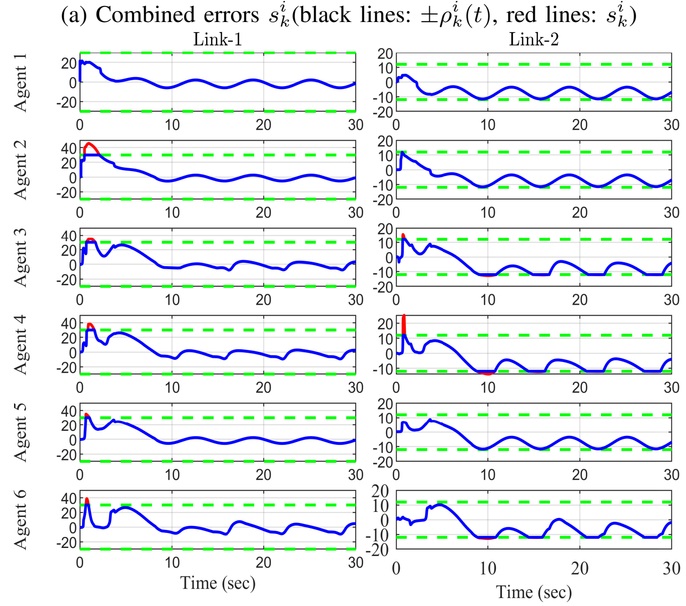

(b) Input signals (red solid line: u_k^i, blue solid lines: τ_k^i, green dotted lines: $\pm\bar{u}_k^i$)

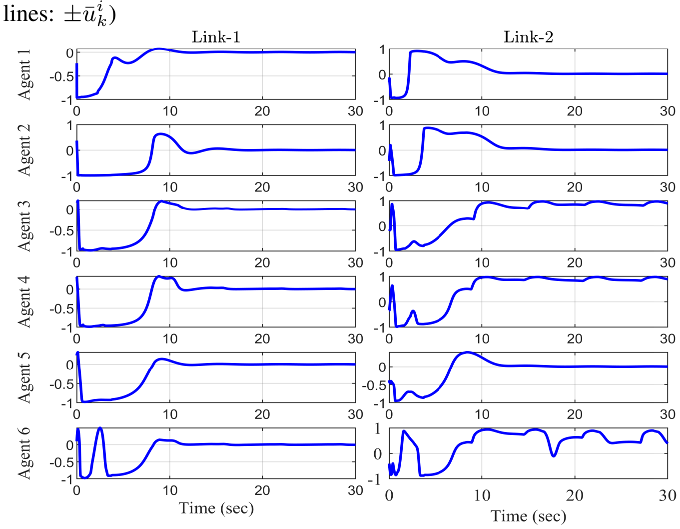

(c) Normalized errors ξ_{sk}^i

Figure 3: System performance of Interconnection 2 for the proposed control.

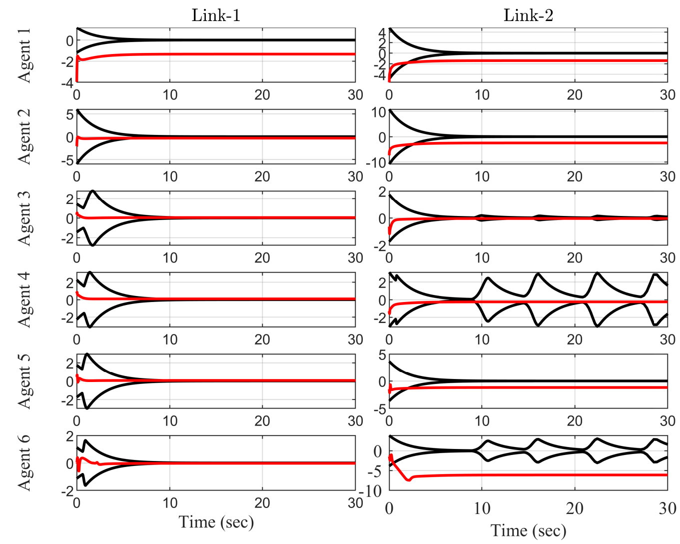

(a) Combined errors s_k^i (black lines: $\pm\rho(t)_k^i$, red lines: s_k^i)

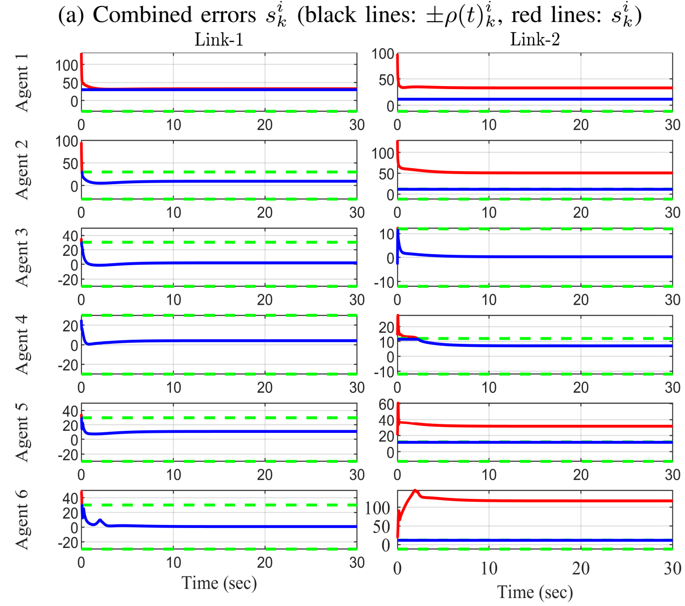

(b) Input signals (red solid line: u_k^i, blue solid lines: τ_k^i, green dotted lines: $\pm\bar{u}_k^i$)

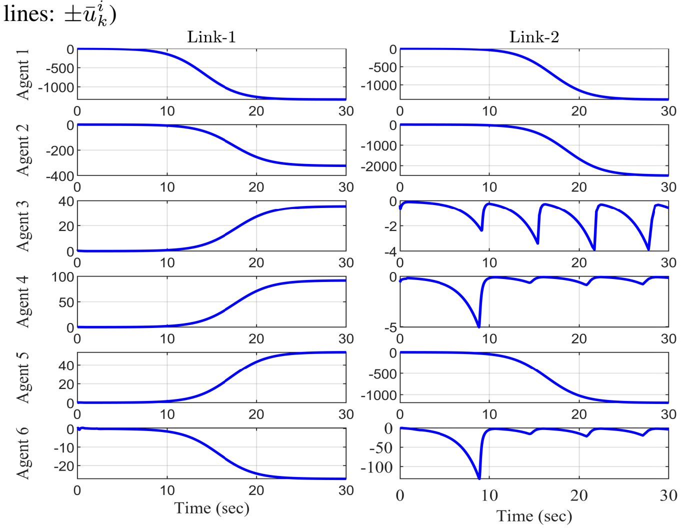

(c) Normalized errors ξ_{sk}^i

Figure 4: System performance of Interconnection 1 for adaptive sliding mode control [31].

Appendix

$$
e = \begin{bmatrix} e_1^1 \\ \vdots \\ e_n^1 \\ e_1^2 \\ \vdots \\ e_n^2 \\ \vdots \\ e_1^N \\ \vdots \\ e_n^N \end{bmatrix}
= \begin{bmatrix}
\sum\limits_{j=2}^{N} a_{1j} & \dots & 0 & -a_{12} & \dots & 0 & \dots & -a_{1N} & \dots & 0 \\
\vdots & \ddots & \vdots & \vdots & \ddots & \vdots & \dots & \vdots & \ddots & \vdots \\
0 & \dots & \sum\limits_{j=2}^{N} a_{1j} & 0 & \dots & -a_{12} & \dots & 0 & \dots & -a_{1N} \\
-a_{21} & \dots & 0 & \sum\limits_{j=1, j\neq 2}^{N} a_{2j} & \dots & 0 & \dots & -a_{2N} & \dots & 0 \\
\vdots & \ddots & \vdots & \vdots & \ddots & \vdots & \dots & \vdots & \ddots & \vdots \\
0 & \dots & -a_{21} & 0 & \dots & \sum\limits_{j=1, j\neq 2}^{N} a_{2j} & \dots & 0 & \dots & -a_{2N} \\
\vdots & \dots & \vdots & \vdots & \dots & \vdots & \dots & \vdots & \dots & \vdots \\
-a_{N1} & \dots & 0 & -a_{N2} & \dots & 0 & \dots & \sum\limits_{j=1, j\neq N}^{N-1} a_{Nj} & \dots & 0 \\
\vdots & \ddots & \vdots & \vdots & \ddots & \vdots & \dots & \vdots & \ddots & \vdots \\
0 & \dots & -a_{N1} & 0 & \dots & -a_{N2} & \dots & 0 & \dots & \sum\limits_{j=1, j\neq N}^{N-1} a_{Nj}
\end{bmatrix}
\begin{bmatrix} q_1^1 \\ \vdots \\ q_n^1 \\ q_1^2 \\ \vdots \\ q_n^2 \\ \vdots \\ q_1^N \\ \vdots \\ q_n^N \end{bmatrix}
$$

$$
+ \begin{bmatrix}
b_1 & \dots & 0 & 0 & \dots & 0 & \dots & 0 & \dots & 0 \\
\vdots & \ddots & \vdots & \vdots & \ddots & \vdots & \dots & \vdots & \ddots & \vdots \\
0 & \dots & b_1 & 0 & \dots & 0 & \dots & 0 & \dots & 0 \\
0 & \dots & 0 & b_2 & \dots & 0 & \dots & 0 & \dots & 0 \\
\vdots & \ddots & \vdots & \vdots & \ddots & \vdots & \dots & \vdots & \ddots & \vdots \\
0 & \dots & 0 & 0 & \dots & b_2 & \dots & 0 & \dots & 0 \\
\vdots & \dots & \vdots & \vdots & \dots & \vdots & \dots & \vdots & \dots & \vdots \\
0 & \dots & 0 & 0 & \dots & 0 & \dots & b_N & \dots & 0 \\
\vdots & \ddots & \vdots & \vdots & \ddots & \vdots & \dots & \vdots & \ddots & \vdots \\
0 & \dots & 0 & 0 & \dots & 0 & \dots & 0 & \dots & b_N
\end{bmatrix}
\left(\begin{bmatrix} q_1^1 \\ \vdots \\ q_n^1 \\ q_1^2 \\ \vdots \\ q_n^2 \\ \vdots \\ q_1^N \\ \vdots \\ q_n^N \end{bmatrix}
- \begin{bmatrix} q_1^0 \\ \vdots \\ q_n^0 \\ q_1^0 \\ \vdots \\ q_n^0 \\ \vdots \\ q_1^0 \\ \vdots \\ q_n^0 \end{bmatrix} \right)
$$

$$
\begin{aligned}
&= (\mathcal{L} \otimes I_n) q + (B \otimes I_n)(q - \underline{1}_N \otimes q^0) \\
&= (\mathcal{L} \otimes I_n)(q - \underline{1}_N \otimes q^0) + (B \otimes I_n)(q - \underline{1}_N \otimes q^0) \\
&= \Big((\mathcal{L} + B) \otimes I_n\Big)(q - \underline{1}_N \otimes q^0) = \Big((\mathcal{L} + B) \otimes I_n\Big)(q - \underline{q}^0) = \Big((\mathcal{L} + B) \otimes I_n\Big)\delta
\end{aligned}
$$

References

[1] C. P. Bechlioulis and G. A. Rovithakis, "Robust adaptive control of feedback linearizable mimo nonlinear systems with prescribed performance," *IEEE Transactions on Automatic Control*, vol. 53, no. 9, pp. 2090–2099, 2008.

[2] T. Berger, M. Puche, and F. L. Schwenninger, "Funnel control for a moving water tank," *Automatica*, vol. 135, p. 109999, 2022.

[3] M. Sewlia, C. K. Verginis, and D. V. Dimarogonas, "Cooperative object manipulation under signal temporal logic tasks and uncertain dynamics," *IEEE Robotics and Automation Letters*, vol. 7, no. 4, pp. 11 561–11 568, 2022.

[4] Z. Liu, Z. Lu, Z. Zhao, M. Ö. Efe, and K.-S. Hong, "Single parameter adaptive neural network control for multi-agent deployment with prescribed tracking performance," *Automatica*, vol. 156, p. 111207, 2023.

[5] T. Berger, "Tracking with prescribed performance for linear non-minimum phase systems," *Automatica*, vol. 115, p. 108909, 2020.

[6] C. K. Verginis and D. V. Dimarogonas, "Asymptotic tracking of second-order nonsmooth feedback stabilizable unknown systems with prescribed transient response," *IEEE Transactions on Automatic Control*, vol. 66, no. 7, pp. 3296–3302, 2021.

[7] A. Theodorakopoulos and G. A. Rovithakis, "Low-complexity prescribed performance control of uncertain mimo feedback linearizable systems," *IEEE Transactions on Automatic Control*, vol. 61, no. 7, pp. 1946–1952, 2015.

[8] R. Ma, L. Fu, and J. Fu, "Prescribed-time tracking control for nonlinear systems with guaranteed performance," *Automatica*, vol. 146, p. 110573, 2022.

[9] J. Zhang, J. Yang, Z. Zhang, and Y. Wu, "Prescribed performance control of Euler-Lagrange systems with input saturation and output constraints," *International Journal of Adaptive Control and Signal Processing*, vol. 36, no. 12, pp. 3184–3204, 2022.

[10] Y. Shi, B. Yi, W. Xie, and W. Zhang, "Enhancing prescribed performance of tracking control using monotone tube boundaries," *Automatica*, vol. 159, p. 111304, 2024.

[11] W. Shi, M. Hou, and G. Duan, "A preset-trajectory-based singularity-free preassigned performance control approach," vol. 69, no. 9, pp. 6183–6190, 2024.

[12] W. Hu and Y. Yang, "Performance guaranteed consensus tracking for double-integrator multi-agent systems via high-dimensional error norm specification," *IEEE Transactions on Industrial Informatics*, vol. 20, no. 9, pp. 11 438–11 448, 2024.

[13] F. Mehdifar, C. P. Bechlioulis, F. Hashemzadeh, and M. Baradarannia, "Prescribed performance distance-based formation control of multi-agent systems," *Automatica*, vol. 119, p. 109086, 2020.
[14] C. P. Bechlioulis and G. A. Rovithakis, "Decentralized robust synchronization of unknown high order nonlinear multi-agent systems with prescribed transient and steady state performance," *IEEE Transactions on Automatic Control*, vol. 62, no. 1, pp. 123–134, 2016.
[15] Z. Guo, D. Henry, J. Guo, Z. Wang, J. Cieslak, and J. Chang, "Control for systems with prescribed performance guarantees: An alternative interval theory-based approach," *Automatica*, vol. 146, p. 110642, 2022.
[16] L. Macellari, Y. Karayiannidis, and D. V. Dimarogonas, "Multi-agent second order average consensus with prescribed transient behavior," *IEEE Transactions on Automatic Control*, vol. 62, no. 10, pp. 5282–5288, 2017.
[17] T. Tao, S. Roy, and S. Baldi, "Stable adaptation in multi-area load frequency control under dynamically-changing topologies," *IEEE Transactions on Power Systems*, vol. 36, no. 4, pp. 2946–2956, 2020.
[18] L. Zhang, C. Deng, W.-W. Che, and L. An, "Adaptive backstepping control for nonlinear interconnected systems with prespecified-performance-driven output triggering," *Automatica*, vol. 154, p. 111063, 2023.
[19] N. Hopfe, A. Ilchmann, and E. Ryan, "Funnel Control With Saturation: Linear MIMO Systems," *IEEE Transactions on Automatic Control*, vol. 55, no. 2, pp. 532–538, 2010.
[20] Y. Yao, X. Liang, Y. Kang, Y. Zhao, J. Tan, and L. Gu, "Dual flexible prescribed performance control of input saturated high-order nonlinear systems," *IEEE Transactions on Cybernetics*, 2025.
[21] Y. Yao, Y. Kang, Y. Zhao, P. Li, and J. Tan, "Flexible prescribed performance output feedback control for nonlinear systems with input saturation," *IEEE Transactions on Fuzzy Systems*, 2024.
[22] Y. Yao, Y. Kang, Y. Zhao, J. Tan, L. Gu, and G. Shi, "Sliding flexible prescribed performance control for input saturated nonlinear systems," *IEEE Transactions on Fuzzy Systems*, 2024.
[23] L. N. Bikas and G. A. Rovithakis, "Prescribed performance under input saturation for uncertain strict-feedback systems: A switching control approach," *Automatica*, vol. 165, p. 111663, 2024.
[24] P. K. Mishra and P. Jagtap, "Approximation-free prescribed performance control with prescribed input constraints," *IEEE Control Systems Letters*, vol. 7, pp. 1261–1266, 2023.
[25] F. Fotiadis and G. A. Rovithakis, "Input-constrained prescribed performance control for high-order mimo uncertain nonlinear systems via reference modification," *IEEE Transactions on Automatic Control*, vol. 69, no. 5, pp. 3301–3308, 2023.
[26] K. Yong, M. Chen, Y. Shi, and Q. Wu, "Flexible performance-based robust control for a class of nonlinear systems with input saturation," *Automatica*, vol. 122, p. 109268, 2020.
[27] Y. Yang, J. Tan, and D. Yue, "Prescribed performance tracking control of a class of uncertain pure-feedback nonlinear systems with input saturation," *IEEE Transactions on Systems, Man, and Cybernetics: Systems*, vol. 50, no. 5, pp. 1733–1745, 2018.
[28] J. Hu, S. Trenn, and X. Zhu, "Funnel control for relative degree one nonlinear systems with input saturation," in *2022 European Control Conference (ECC)*. London, United Kingdom: IEEE, 2022, pp. 227–232.
[29] P. S. Trakas and C. P. Bechlioulis, "Approximation-free adaptive prescribed performance control for unknown siso nonlinear systems with input saturation," in *2022 IEEE 61st Conference on Decision and Control (CDC)*. Cancun, Mexico: IEEE, 2022, pp. 4351–4356.
[30] ——, "Robust adaptive prescribed performance control for unknown nonlinear systems with input amplitude and rate constraints," *IEEE Control Systems Letters*, vol. 7, pp. 1801–1806, 2023.
[31] K. Shao, R. Tang, F. Xu, X. Wang, and J. Zheng, "Adaptive sliding mode control for uncertain Euler-Lagrange systems with input saturation," *Journal of the Franklin Institute*, vol. 358, no. 16, pp. 8356–8376, 2021.
[32] W. Cheng, H. Xue, H. Liang, and W. Wang, "Prescribed performance adaptive fuzzy control of stochastic nonlinear multi-agent systems with input hysteresis and saturation," *International Journal of Fuzzy Systems*, vol. 24, no. 1, pp. 91–104, 2022.
[33] M. Mesbahi, *Graph theoretic methods in multiagent networks*. Princeton University Press, 2010.
[34] R. A. Horn and C. R. Johnson, *Matrix analysis*. Cambridge, UK: Cambridge University Press, 2012.
[35] M. Lu, L. Liu, and G. Feng, "Adaptive tracking control of uncertain Euler–Lagrange systems subject to external disturbances," *Automatica*, vol. 104, pp. 207–219, 2019.
[36] M. W. Spong, S. Hutchinson, and M. Vidyasagar, *Robot modeling and control*. John Wiley & Sons, 2020.
[37] J.-J. E. Slotine, W. Li *et al.*, *Applied nonlinear control*. Prentice hall Englewood Cliffs, NJ, 1991.
[38] C. P. Bechlioulis and G. A. Rovithakis, "A low-complexity global approximation-free control scheme with prescribed performance for unknown pure feedback systems," *Automatica*, vol. 50, no. 4, pp. 1217–1226, 2014.
[39] E. D. Sontag, *Mathematical control theory: deterministic finite dimensional systems*. Springer Science & Business Media, 2013.
[40] C. Makkar, G. Hu, W. G. Sawyer, and W. E. Dixon, "Lyapunov-based tracking control in the presence of uncertain nonlinear parameterizable friction," *IEEE Transactions on Automatic Control*, vol. 52, no. 10, pp. 1988–1994, 2007.
[41] H. Kimura, Y. Fukuoka, and A. H. Cohen, "Biologically inspired adaptive walking of a quadruped robot," *Philosophical Transactions of the Royal Society A: Mathematical, Physical and Engineering Sciences*, vol. 365, no. 1850, pp. 153–170, 2007.

Tian Tao is a postdoctoral researcher at the Division of Decision and Control Systems, School of Electrical Engineering and Computer Science, KTH Royal Institute of Technology. She received the B.S. in Electrical Engineering & Automation from Wuhan Polytechnic University, China in 2013, the M.S. in Automation Engineering from the University of Electronic Science and Technology of China in 2018 and the Ph.D. in Systems and Control from Delft University of Technology, The Netherlands in 2022. Her research interests are adaptive control, switching topologies, prescribed performance control of multi-agent and interconnected systems.

Charalampos P. Bechlioulis was born in Arta, Greece, in 1983. He received the diploma degree (first in his class) in electrical and computer engineering, the bachelor of science degree (second in his class) in mathematics, and the Ph.D. degree in electrical and computer engineering from the Aristotle University of Thessaloniki, Thessaloniki, Greece, in 2006, 2011, and 2011, respectively. He is currently an Associate Professor with the Division of Systems and Control, Department of Electrical and Computer Engineering, University of Patras, Patras, Greece. He has authored more than 100 papers in scientific journals and conference proceedings and three book chapters. His research interests include nonlinear control with prescribed performance, system identification, control of robotic vehicles, and multiagent systems.

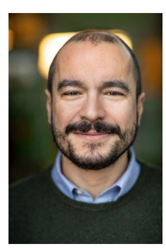

Dimos V. Dimarogonas (Fellow, IEEE) was born in Athens, Greece, in 1978. He received the Diploma degree in electrical and computer engineering and the Ph.D. degree in mechanical engineering from the National Technical University of Athens, Athens, Greece, in 2001 and 2007, respectively. From 2007 to 2010, he was a Postdoctoral Researcher with the Department of Automatic Control, KTH Royal Institute of Technology, Stockholm, Sweden, and the Laboratory for Information and Decision Systems, Massachusetts Institute of Technology, Cambridge, MA, USA. He is currently a Professor with the Division of Decision and Control Systems, School of Electrical Engineering and Computer Science, KTH Royal Institute of Technology. His research interests include multiagent systems, hybrid systems and control, robot navigation and manipulation, human–robot interaction, and networked control. Dr. Dimarogonas is in the Editorial Board of the Automatica and IEEE Transactions on Control of Network Systems. He was a recipient of the ERC Starting Grant in 2014, the ERC Consolidator Grant in 2019, and the Knut och Alice Wallenberg Academy Fellowship in 2015.